Available online at www.sciencedirect.com

SciVerse ScienceDirect

Journal of the European Ceramic Society 32 (2012) 2121–2127

www.elsevier.com/locate/jeurceramsoc

Macroporous sol–gel hydroxyapatite moulding via confinement into shaped acrylate–acrylamide copolymers

Mercedes Vila [a,b], Tatiana Fernández-Lanas [a,b], Blanca González [a,b], María Vallet-Regí [a,b,*]

[a] *Departamento de Química Inorgánica y Bioinorgánica, Facultad de Farmacia, Universidad Complutense de Madrid, Plaza de Ramón y Cajal s/n, 28040 Madrid, Spain*

[b] *Networking Research Center on Bioengineering, Biomaterials and Nanomedicine (CIBER-BBN), Spain*

Received 19 October 2011; received in revised form 10 January 2012; accepted 26 January 2012
Available online 11 March 2012

Abstract

Polyacrylate salts and polyacrylamide have been extensively used for absorbing and/or retaining large amounts of water and/or ionic species. Herein, we propose the use of this polymers' swelling capability as a new way to obtain porous spheres of nanocrystalline hydroxyapatite (HA). Macroporous nanostructured HA with a pore size between 1 and 500 μm is obtained when using the hydrogel as template. The removal of the organic template gives rise to the material in the form of a sphere which size and shape can be determined by the template contour. The use of this type of polymer constitutes not only an easy way to obtain HA beads but it would be also possible to form scaffolds with different shapes and sizes due to the versatility of the polymer. Degradation and bioactivity tests of the ceramic material have been performed showing an enhanced bioactivity and a suitable degradation rate to be applied in bone tissue engineering.

Keywords: Sol–gel processes; Biomedical applications; Apatite; Shaping; Porous ceramics

1. Introduction

It has been widely discussed the importance of a hierarchical porosity in an implantable material for bone regeneration processes. This property is important to enhance the functionability of the material for tissue regeneration, allowing from fluid exchange up to cell permeability along the surfaces.[1]

Synthetic calcium phosphates, in particular hydroxyapatite (HA), are the most commonly used ceramics in dentistry and bone repair applications since they show a very good performance due to its similarity with the inorganic component of the bone.[2–4] Nowadays materials structure, as well as biological performance, can be controlled by means of modulating the synthesis conditions. One of the aims in bone tissue engineering is to produce HA with nanometer size crystals that mimic the reactivity of natural bone. But it is also true that there is still a big challenge in how to obtain, in an easy and affordable way, implantable scaffolds with the right porosity, size and complicated shapes.

On the other hand, polymer science and its development provide affordable solutions in the biomaterials field.[5] For instance, the layer-by-layer (LbL) assembly technique has been used to produce polymer hydrogel capsules as therapeutic carriers for controlled drug delivery. The LbL-assembled material is usually formed by deposition of interacting polymers onto a sacrificial colloidal template that is finally removed by dissolution or chemical processes.[6,7] Another approach makes use of close-packed polymer spheres that act as template for three-dimensionally ordered macroporous materials. In this line, a sol–gel derived hydroxyapatite-containing calcium phosphate has been obtained after filling the interstitial spaces of the colloidal crystal with a precursor solution and, subsequently, the removal of the polymer template is performed by calcinations.[8] Finally, the synthesis of porous ceramic beads or ceramic pieces of complex shapes for use as materials for tissue regeneration

* Corresponding author.
E-mail addresses: mvila@farm.ucm.es (M. Vila), vallet@farm.ucm.es (M. Vallet-Regí).

0955-2219/$ – see front matter © 2012 Elsevier Ltd. All rights reserved.
doi:10.1016/j.jeurceramsoc.2012.01.034

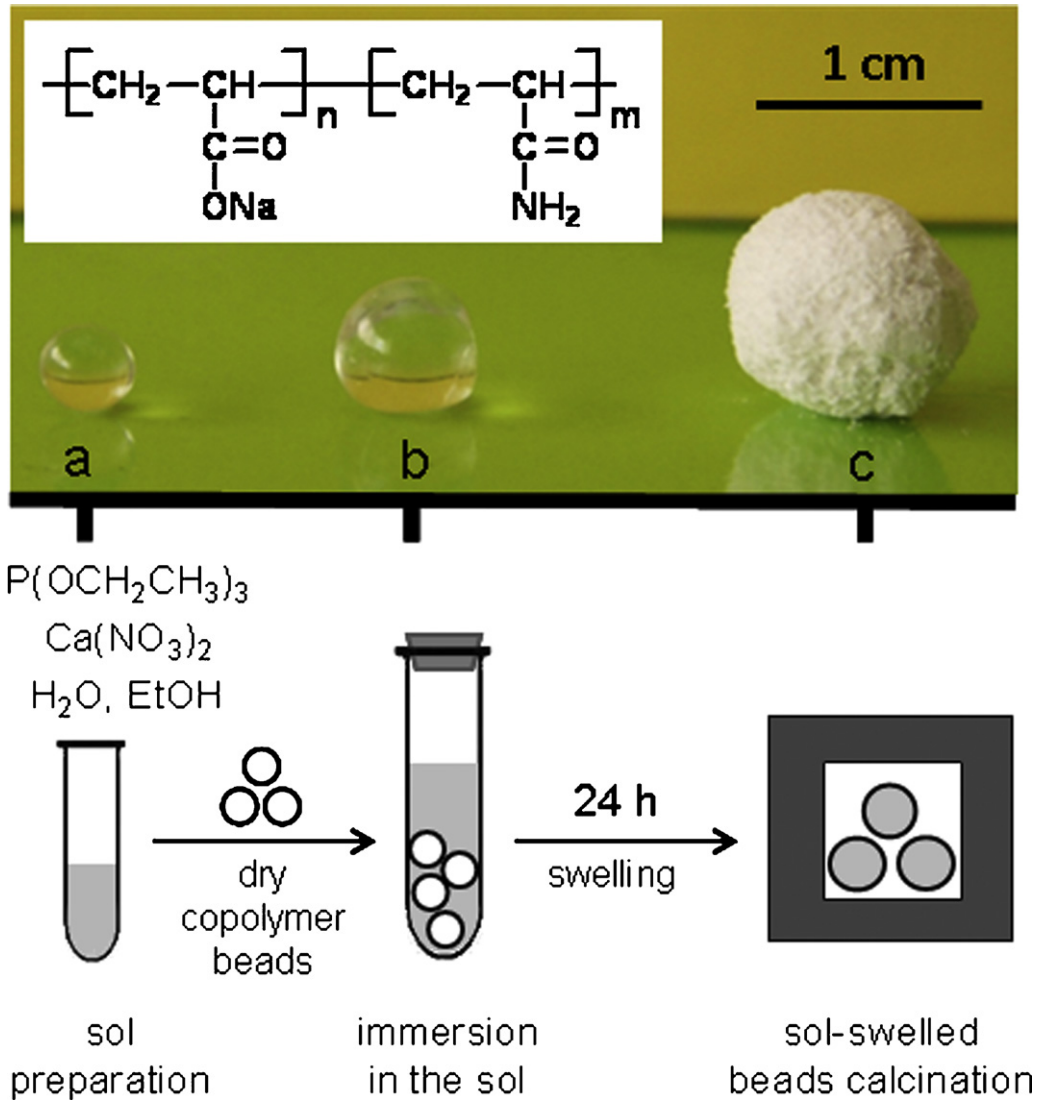

Fig. 1. Digital photography of (a) dry polymer beads, (b) sol swelled polymer beads and (c) final porous HA bead. Inset: chemical structure of sodium acrylate–acrylamide copolymer. Down: scheme of the synthetic procedure followed for the templated ceramic sphere.

is of great interest.[9] Hierarchically three-dimensional porous bioactive glass ceramic beads have been fabricated by the triblock copolymer self-assembly and sol–gel techniques.[10,11]

In addition, the use of hydrogels for different biomedical purposes is extensive and diverse. Hydrogels such as acrylate and acrylamide based polymers have been investigated as potential carriers for drug[12,13] and antibiotic local delivery,[14] field of growing interest, as well as cartilage substitutes.[15] Polyacrylate salts and polyacrylamide have been extensively used for retaining or absorbing large amounts of water or ionic species.[16–18] This type of hydrogel swelling capacity is exhibited when it is immersed in aqueous media, which as has a high dielectric constant. The mechanism for the swelling behaviour can be explained by the repulsion created between the polymer carboxylate groups. There is an ionic environment created when the carboxylic groups of the polymer are dissociated in the aqueous medium. These groups are capable of generate ionic charges along the polymeric chain which provokes electrostatic repulsion between them and, therefore, the subsequently expansion. This situation also causes the absorption of external ionic species, which compensates the osmotic pressure in order to get electroneutrality.[19] The interesting behaviour of this type of polymeric substances attracted our attention as a possible template for our ceramic materials.

In the present work, we propose a new method to obtain nanocrystalline hydroxyapatite scaffolds in the form of beads without any central cavity and with a porosity ranging between 1 and 500 μm, using a hydrogel as the sphere template. The removal of the template gives rise to the macroporous nanostructured HA formed sphere and the size and shape of such material can be determined by the template shape. It must be highlighted that the use of this kind of polymer constitutes not only an easy way to obtain beads but, moreover, it is also possible to get scaffolds with different shapes and sizes due to the versatility of the polymer.

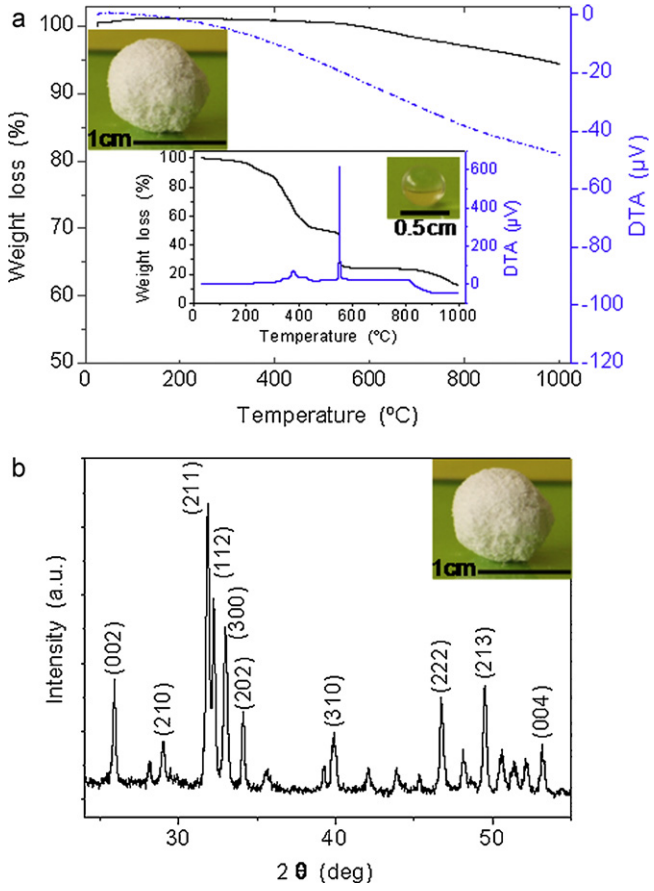

Fig. 2. (a) Thermogravimetric and differential thermal analyses of HA spheres. Inset: TGA and DTA curves of sodium acrylate–acrylamide copolymer. (b) Powder X-ray diffraction pattern of the ceramic bead.

2. Experimental

2.1. Reagents and equipment

Triethyl phosphite (TIP) and calcium nitrate tetrahydrate were purchased from Sigma–Aldrich. These compounds were used without further purification. Deionized water was further purified by passage through a Milli-Q Advantage A-10 Purification System (Millipore Corporation) to a final resistivity of 18.2 MΩ cm. All other chemicals (absolute ethanol, sodium chloride and the other reagents for the preparation of simulated body fluid (SBF) and Ringer's solution) were of the best quality commercially available and used as received.

Insoluble high molecular weight sodium acrylate–acrylamide copolymer, manufactured as 0.3 cm diameter beads, was used as template. Characterization of the polymer beads to confirm structure and purity was performed by means of elemental analysis and ^{1}H and ^{13}C high resolution magic angle spinning nuclear magnetic resonance (HR-MAS NMR) and energy dispersive X-ray (EDX) spectroscopies. A molar% composition of $(CH_2CHCOOH)_{27}(CH_2CHCOONa)_{34}(CH_2CHCONH_2)_{39}$ was obtained.

HR-MAS NMR spectra were obtained on a Bruker AMX500MHz spectrometer equipped with a semisolid state

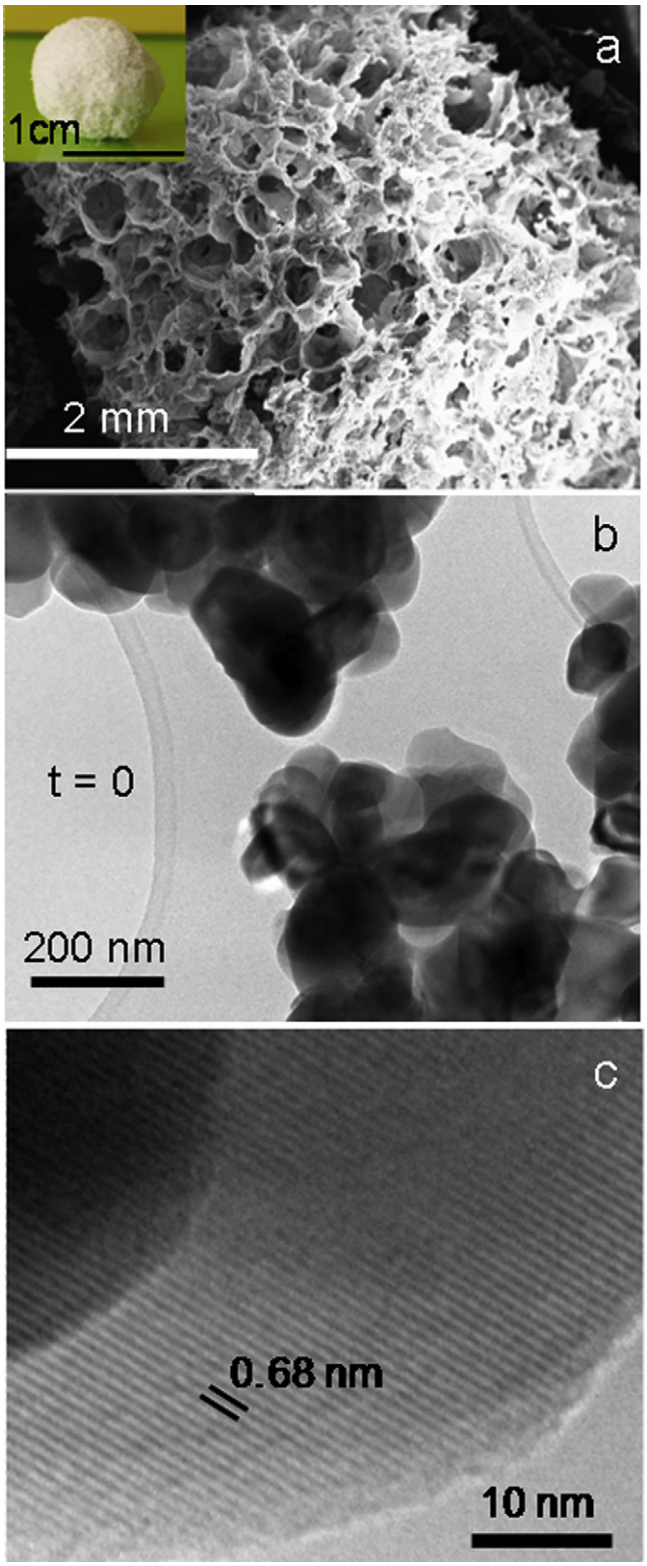

Fig. 3. (a) SEM micrograph of a cross section of the ceramic spheres. Inset: ceramic bead. (b) TEM image of HA spheres and (c) high resolution TEM of a HA crystallite.

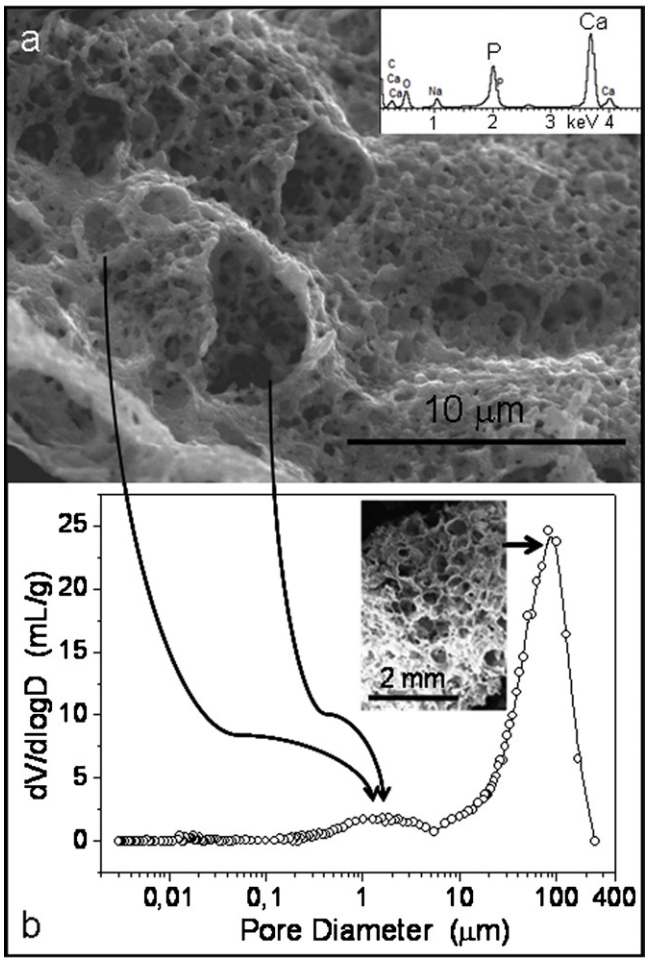

Fig. 4. (a) SEM micrograph of the ceramic spheres. EDX analysis is displayed as inset. (b) Pore size distribution of ceramic spheres obtained by Hg intrusion porosimetry. Inset: SEM micrograph of the ceramic spheres at different magnification.

probe. Measurements were performed in the gel state, by swelling the polymers with D_2O to a concentration of *ca.* 100 mg/mL.

X-ray powder diffraction (XRD) data were collected on a Philips X'Pert Plus diffractometer (Philips Electronics NV, Eindhoven, Netherlands) with Bragg–Brentano geometry, operating with CuKα radiation (λ = 1.5406 Å) at 40 kV and 20 mA. The diffractograms were collected over the range between 20° and 60° 2θ with a step size of 0.02° and an acquisition time of 10 s per step.

Scanning electron microscopy (SEM) was performed using a 40 kV JEOL JSM 6400 with a 35 Å resolution and equipped with an Oxford Link EDX probe.

Surface area measurements of the ceramic materials were carried out by nitrogen adsorption/desorption analyses performed at 77 K using an ASAP 2020 porosimeter (Micromeritics Co., Norcross, GA, USA). Prior to the analysis powdered samples were degassed at 80 °C for 24 h under a vacuum lower than 10^{-5} Torr. The surface area was determined by the Brunauer–Emmett–Teller (BET) method.[20] A mercury intrusion porosimetry study was carried out to determine the total porosity and the pore size distribution of the spheric samples, using a Micromeritics (Norcross, GA) AutoPore IV 9500 mercury porosimeter.

Chemical microanalyses were performed with a Perkin Elmer 2400 CHN thermo analyzer. Thermogravimetric analysis (TGA) and differential thermal analysis (DTA) were carried out in air between 30 and 1000 °C with a flow rate of 100 mL/min and a heating rate of 5 °C/min using a Perkin Elmer Pyris Diamond thermobalance.

Transmission electron microscopy (TEM) assays of ground samples were carried out in a JEOL 3000 FEG microscope operating at 300 kV (*C*s 0.6 mm, resolution 1.7 Å) and fitted with a double tilting goniometer stage (±45°) and an Oxford LINK EDX analyzer.

2.2. Synthesis of the ceramic beads

The ceramic material was prepared via the sol–gel method.[21] The phosphorous precursor, $P(OCH_2CH_3)_3$, was hydrolyzed in a molar ratio TIP/H_2O of 1:4, under continuous stirring during 24 h and subsequently diluted in ethanol in a relation 1:5 (v/v) and stirred for 30 min. Then, a 4 M $Ca(NO_3)_2{\cdot}4H_2O$ aqueous solution was added in order to obtain the Ca/P molar ratio of 1.67, which corresponds to the HA phase.[22] After 15 min, the sol was taken to 60 °C for aging during 6 h. Then, a second dilution in ethanol, to double the sol volume, was performed. At this time, the polymer beads were immersed in a surplus of sol and treated at 60 °C during 24 h resulting in an increase of the sphere's volume to its maximum. Finally, ceramic spheres were obtained by means of an annealing process of the system in air at 700 °C during 8 h, to remove all the organic compounds and synthesize the ceramic phase.

2.3. In vitro assays

The stability tests were performed by soaking the spheres in Ringer's solution.[23] To prepare the Ringer's solution KCl (0.3 g), $CaCl_2$ (0.2 g), NaCl (6 g) and sodium DL-lactate (3.1 g), as buffer, were dissolved in 1 l of deionized water. Samples were immersed in 40 ml of the Ringer's solution at 37 °C and placed in an orbital shaker at 70 rpm.

The assessment of *in vitro* bioactivity assays of the samples was carried out by soaking the spheres, held over platinum holders, in a volume of SBF determined by the equation $S_{monolith}$ (cm^2)/V_{SBF} (cm^3) = 0.075 cm^{-1}, at 37 °C and at physiological pH of 7.4. SBF is an acellular aqueous solution proposed by Kokubo et al.[24–26] with inorganic ion composition almost equal to that of human plasma.

To avoid microorganism contamination, the SBF and Ringer's solutions were previously filtered with a 0.22 μm Millipore System, and all manipulations of the pieces and solutions were done in a laminar flux cabinet Telstar AV-100. After different periods of time in SBF or Ringer's solution (5 h, 25 h, 5 days, 14 days and 29 days), the samples were removed from the fluid, thoroughly rinsed with water and ethanol, and dried in air at room temperature. The variations of Ca^{2+} concentration and

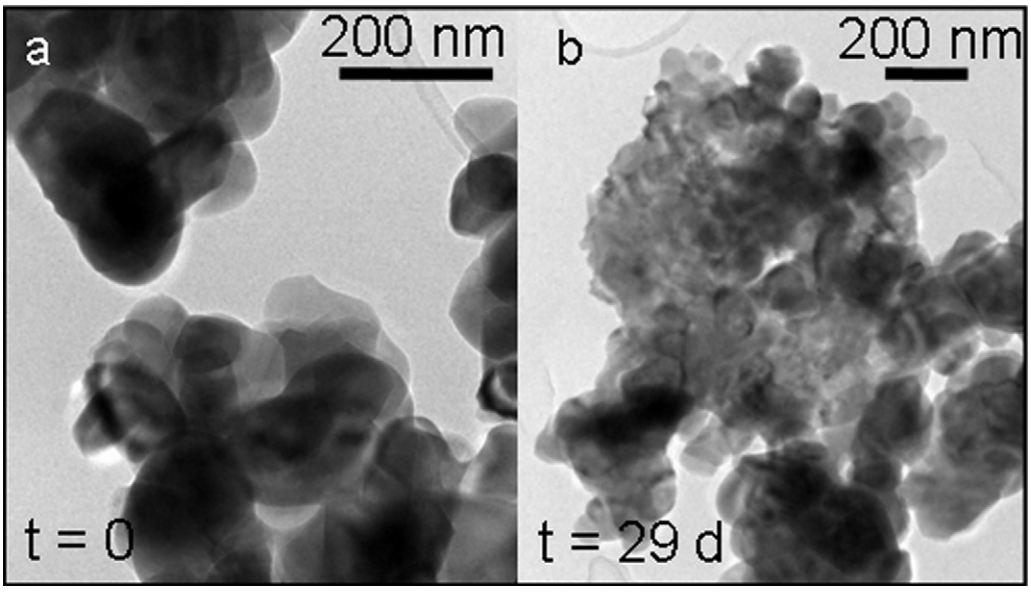

Fig. 5. (a) TEM images of HA spheres before ($t = 0$) and (b) after immersion in Ringer's solution for 29 days ($t = 29$ days).

pH in solution were determined with an ILyte Na^+, K^+, Ca^{2+}, pH analyzer, and the variations in the sample were characterized by TEM.

3. Results and discussion

3.1. Preparation and characterization of the ceramic spheres

During the synthetic process (scheme in Fig. 1) the copolymer beads are immersed in the calcium phosphate precursor solution, at the stage of sol. Then, a swelling process caused by the repulsion created between the polymer carboxylate groups and the absorption of the sol, takes place in a few hours, resulting in an enlargement of the beads size although their geometry is maintained, as it can be seen in Fig. 1a and b. Although the complete swelling of the polymer takes place in *ca.* 8 h, the beads were soaked for 24 h in the sol, which is the complete sol aging. With this experimental set up the entire swelling of the polymer is therefore assured. The removal of the polymeric template is subsequently performed by calcination methods giving rise to the shaped ceramic in the form of a sphere with a diameter of *ca.* 1 cm with no internal cavity and a constant morphology and structure along the sphere radius. The calcination of the organic species provokes the production of gases in the form of bubbles and therefore forming the porous structure of the inorganic bead. The shape of the material remains mimicking the template contour but the diameter is increased in more than 300% (see Fig. 1c). The ceramic beads presented good mechanical properties for easy-handling. The entire absence of the copolymer template in the final ceramic spheres after calcination was confirmed by chemical microanalysis as well as thermogravimetric and differential thermal techniques. The organic residue was successfully removed, since there is no weight loss neither exothermic process related to the polymer in the TGA/DTA curves (Fig. 2a), and chemical analysis gave a negligible carbon content. The ceramic phase was analyzed by powder XRD, corresponding the XRD pattern of the ceramic material to a pure HA nanocrystalline phase (Fig. 2b).

The surface morphology characterization of the spheres performed by SEM analysis (Figs. 3a and 4a) shows cancellous structured beads with well interconnected and hierarchically arranged open macropore structures with pore sizes between 50 and 500 μm. The standard less semi-quantitative results from EDX in the ceramic sphere reveal a Ca/P molar ratio of 1.8, suggesting a slightly phosphorous deficient hydroxyapatite but very close to the stoichiometric ratio of 1.67. Crystalline grains of *ca.* 100–150 nm are observed by TEM (Fig. 3b). Fig. 3c shows a TEM image at a higher magnification evidencing the presence of pure HA with a *d*-spacing at 0.68 nm which corresponds to the 001 reflections of an apatite-like phase.

The existence of porosity in the micrometer range was investigated by mercury intrusion porosimetry (Fig. 4b). The ceramic material exhibited a bimodal pore size distribution with an intense and broad maximum centered at *ca.* 90 μm and a low intense maximum around 2 μm, therefore confirming the existence of porosity in the micrometer range between 1 and 300 μm (being 300 μm the maximum range measured in the Hg porosimeter). Moreover, the calculated total porosity of *ca.* 79% is a relatively high value for conformed calcium phosphates. Surface area measurements of the ceramic spheres were made by means of N_2 adsorption analyses. The ceramic matrixes exhibited N_2 adsorption isotherms corresponding to a practically non porous material in the 1–300 nm range with a BET specific surface area of *ca.* 20 m^2/g. The N_2 adsorption analyses of the materials revealed that these materials do not present pores in the mesopore range.

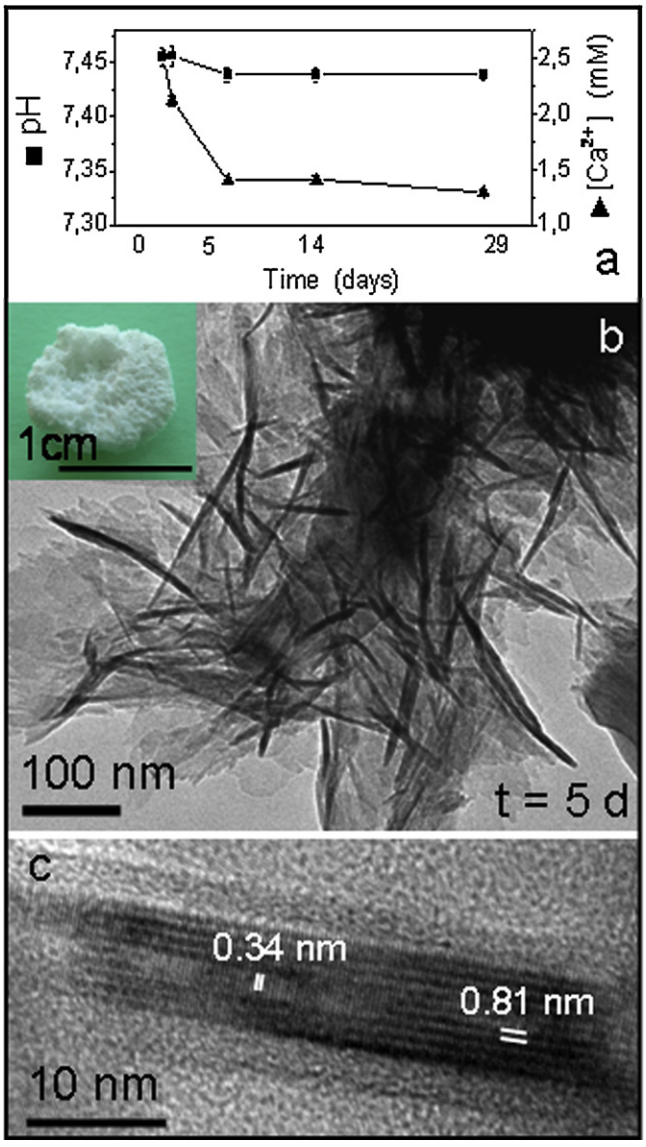

Fig. 6. (a) Variation of the pH and Ca^{2+} concentration in the SBF solution during assay. Error bars represent the standard deviation for four measurements ($N = 4$). (b) TEM images of HA spheres after immersion in SBF for 5 days. Inset: cross-section of a sphere after assay. (c) Representative HRTEM of one of the aciculaes.

3.2. *In vitro* stability and bioactivity evaluation

In order to mimic the behaviour of the ceramic spheres under physiological conditions and to prove their viability as biomaterial, *in vitro* test was performed by soaking them into Ringer and SBF solutions for different periods of time.

Immersion of the HA spheres into Ringer's solution was used to evaluate the stability of the ceramic material under physiological conditions. At the end of the assay ($t = 29$ days) it is observed that the morphological structure of the spheres undergoes in a lower crystal size affecting the bulk of the sphere compared with the initial morphology at $t = 0$, as observed by TEM (see Fig. 5). These facts suggest a sphere's degradation due to a slow decrease of the structural stability as a result of dissolution in the medium.

The viability of the HA spheres as bioactive materials was also *in vitro* tested in SBF for different periods of time up to 29 days. This test gives an idea of the ability of materials to form hydroxycarbonated calcium deficient apatite on their surfaces and it has been widely used for the study of *in vitro* biomineralization of bioactive glasses, also correlated with their *in vivo* performance.[24–26] The pH value was constant at *ca.* 7.4 during the whole assay, however, the Ca^{2+} concentration in the medium decreased from the original value in SBF of 2.5 mM to *ca.* 1.4 mM after 5 days of assay, maintained stable in that value for the rest of the assay (see Fig. 6a). This observation would be in agreement with the possible hydroxyapatite precipitation in the samples and, therefore, it was investigated by TEM. The results showed that after 5 days of immersion (Fig. 6b), the formation of HA crystals on the inner and outer ceramic sphere surfaces can be already detected. A high resolution TEM image (Fig. 6c) shows the structure of one of the aciculae, where the *d*-spacing of 0.81 and 0.34 nm relative to 1 1 0 and 0 0 2 reflections of the HA are detailed. The formation of hydroxyapatite in such a short period of time indicates that this material is able to promote very fast, the precipitation of HA from metastable solutions. This event is probably due to the high porosity of these materials that implies a high exposure of the ceramic material to the medium. HA is a Class B material,[27,28] which are defined to be only osteoconductive materials, allowing bone bonding and growth along their surface with slow kinetics, typical behaviour of dense synthetic calcium phosphates. To the present, there have been efforts to enhance biological response of HA, for example, it has been reported the substitution of carbonate and silicate ions in synthetic HA.[29–31] In this case, the high surface area is enhancing bioactivity response thus accelerating the process of osteoproduction on those surfaces by increasing the kinetics of ion dissolution and surface reactions.

4. Conclusions

Hierarchical porous nanocrystalline hydroxyapatite spheres, with a pore range from 1 to 500 μm, have been obtained via sol–gel by using a copolymer as shaping template. The removal of the template by calcination gives rise to the macroporous nanostructured HA sphere. Moreover, the size and shape of the formed ceramic material are determined by the copolymer outline since the sol-swelled beads retain their shape after eliminating the copolymer template.

It must be highlighted that the use of this type of polymer constitutes not only an easy way to obtain beads, but it would be also possible to form scaffolds of different sizes and shapes due to the versatility of the polymer to be manufactured in different shapes and sizes. Therefore, a reproducible and useful method to perform porous calcium phosphate with a well-defined size and shape has been developed. The proposed method makes use of a polymeric template that can be designed for every specific purpose, avoiding the limitations of ceramic scaffold conformation.

Furthermore, the resulting porous hydroxyapatite materials, with spherical shape in this case, show a good *in vitro* degradation performance and an enhanced *in vitro* bioactivity compare

to synthetic hydroxyapatite, being expected a positive influence on the cells response.

Acknowledgements

This work has been financially supported by the Spanish CICYT through project MAT-2008-00736, by the Spanish National CAM through project S2009/MAT-172. We also thank the X-ray Diffraction C.A.I. and the Electron Microscopy C.A.I. of Universidad Complutense de Madrid. M. Vila thanks the financial support of the Fondo Social Europeo the Ramón y Cajal Program and the Marie Curie FP7-PEOPLE-2007-2-2-ERG.

References

1. Chen QZ, Rezwan K, Françon V, Armitage D, Nazhat SN, Jones FH, et al. Surface functionalization of Bioglass®-derived porous scaffolds. *Acta Biomater* 2007;**3**(4):551–62.
2. Vallet-Regí M, Arcos D. *Biomimetic nanoceramics in clinical use—from materials to applications*. RSC Publishing; 2008.
3. Vallet-Regí M. Evolution of bioceramics within the field of biomaterials. *C R Chim* 2010;**13**(1–2):174–85.
4. Vallet-Regí M, Ruiz-Hernandez E. Bioceramics: from bone regeneration to cancer nanomedicine. *Adv Mater* 2011;**44**:5177–218.
5. Wu D-Q, Qiu F, Wang T, Jiang X-J, Zhang X-Z, Zhuo R-X. Toward the development of partially biodegradable and injectable thermoresponsive hydrogels for potential biomedical applications. *ACS Appl Mater Interfaces* 2009;**1**(2):319–27.
6. De Geest BG, De Koker S, Sukhorukov GB, Kreft O, Parak WJ, Skirtach AG, et al. Polyelectrolyte microcapsules for biomedical applications. *Soft Matter* 2009;**5**(2):282–91.
7. Yan Y, Johnston APR, Dodds SJ, Kamphuis MMJ, Ferguson C, Parton RG, et al. Uptake and intracellular fate of disulfide-bonded polymer hydrogel capsules for doxorubicin delivery to colorectal cancer cells. *ACS Nano* 2010;**4**(5):2928–36.
8. Melde BJ, Stein A. Periodic macroporous hydroxyapatite-containing calcium phosphates. *Chem Mater* 2002;**14**(8):3326–31.
9. Gyger Jr LS, Kulkarni P, Bruck HA, Gupta SK, Wilson Jr OC. Replamineform inspired bone structures (RIBS) using multi-piece molds and advanced ceramic gelcasting technology. *Mater Sci Eng C* 2007;**27**(4):646–53.
10. Yun H-S, Kim S-E, Hyun Y-T. Preparation of bioactive glass ceramic beads with hierarchical pore structure using polymer self-assembly technique. *Mater Chem Phys* 2009;**115**(2–3):670–6.
11. Yun H-S, Park J-W, Kim S-H, Kim Y-J, Jang J-H. Effect of the pore structure of bioactive glass balls on biocompatibility in vitro and in vivo. *Acta Biomater* 2011;**7**(6):2651–60.
12. Tang C, Yin L, Yu J, Yin C, Pei Y. Swelling behavior and biocompatibility of Carbopol-containing superporous hydrogel composites. *J Appl Polym Sci* 2007;**104**(5):2785–91.
13. Schmidt JJ, Rowley J, Kong HJ. Hydrogels used for cell-based drug delivery. *J Biomed Mater Res Part A* 2008;**87A**(4):1113–22.
14. Turos E, Shim J-Y, Wang Y, Greenhalgh K, Reddy GSK, Dickey S, et al. Antibiotic-conjugated polyacrylate nanoparticles: new opportunities for development of anti-MRSA agents. *Bioorg Med Chem Lett* 2007;**17**(1):53–6.
15. Azuma C, Yasuda K, Tanabe Y, Taniguro H, Kanaya F, Nakayama A, et al. Biodegradation of high-toughness double network hydrogels as potential materials for artificial cartilage. *J Biomed Mater Res Part A* 2007;**81**(2):373–80.
16. Myagchenkov VA, Kurenkov VF. Applications of acrylamide polymers and copolymers: a review. *Polym Plast Technol Eng* 1991;**30**(2–3):109–35.
17. Baker BA, Murff RL, Milam VT. Tailoring the mechanical properties of polyacrylamide-based hydrogels. *Polymer* 2010;**51**(10):2207–14.
18. Flood C, Cosgrove T, Espidel Y. Sodium polyacrylate adsorption onto anionic and cationic silica in the presence of salts. *Langmuir* 2007;**23**(11):6191–7.
19. Benda D, Snuparek J, Cermak V. Inverse suspension polymerization of the hydrophilic acrylic monomers in the static continuous phase. *Dispers Sci Technol* 1996;**18**(2):115–21.
20. Kruk M, Jaroniec M, Sayari A. Relations between pore structure parameters and their implications for characterization of mcm-41 using gas adsorption and x-ray diffraction. *Chem Mater* 1999;**11**(2):492–500.
21. Sánchez-Salcedo S, Vila M, Izquierdo-Barba I, Cicuéndez M, Vallet-Regí M. Biopolymer-coated hydroxyapatite foams: a new antidote for heavy metal intoxication. *J Mater Chem* 2010;**20**(33):6956.
22. Elliott JC. Structure and chemistry of the apatites and other calcium orthophosphates. In: *Studies in inorganic chemistry, vol. 18*. Amsterdam: Elsevier; 1994. p. 59.
23. Kohri M, Miki K, Waite DE, Nakajima H, Okabe T. In vitro stability of biphasic calcium phosphate ceramics. *Biomaterials* 1993;**14**(4):299–304.
24. Kokubo T, Kushitani H, Sakka S, Kitsugi T, Yamamuro T. Solutions able to reproduce in vivo surface–structure changes in bioactive glass–ceramic A-W3. *J Biomed Mater Res Part A* 1990;**24**(6):721–34.
25. Kokubo T. Design of bioactive bone substitutes based on biomineralization process. *Mater Sci Eng C* 2005;**25**(2):97–104.
26. Kokubo T, Takadama H. How useful is SBF in predicting in vivo bone bioactivity? *Biomaterials* 2006;**27**(15):2907–15.
27. Hench LL. Bioactive ceramics: theory and clinical applications. In: Andersson OH, Yli-Urpo A, editors. *Bioceramics*. 7th ed. Oxford, England: Butterworth-Heinemann Ltd.; 1994. p. 1–3.
28. Hench LL, Wheeler DL, Greenspan DC. Molecular control of bioactivity in sol–gel glasses. *J Sol–Gel Sci Technol* 1998;**13**(1–3):245–50.
29. Carlisle EM. Silicon: a possible factor in bone calcification. *Science* 1970;**167**(3916):279–80.
30. Arcos D, Rodríguez-Carvajal J, Vallet-Regí M. Silicon Incorporation in Hydroxylapatite Obtained by Controlled Crystallization. *Chem Mater* 2004;**16**(11):2300–8.
31. Hing KA, Revell PA, Smith N, Buckland T. Effect of silicon level on rate, quality and progression of bone healing within silicate-substituted porous hydroxyapatite scaffolds. *Biomaterials* 2007;**27**(29):5014–26.